All-optical switching in a high-Q Fabry–Perot cavity filled with a quadratic material

G. D'Aguanno

Istituto Nazionale Fisíca della Materia, Dipartimento di Energetica, Università di Roma "La Sapienza," Via A. Scarpa, 16, I-00161 Rome, Italy, and
Weapons Sciences Directorate, AMSMI-RD-WS, Development and Engineering Center, U.S. Army Missile Command, Building 7804, Redstone Arsenal, Alabama 35898-5000

E. Angelillo and C. Sibilia

Istituto Nazionale Fisíca della Materia, Dipartimento di Energetica, Università di Roma "La Sapienza," Via A. Scarpa, 16, I-00161 Rome, Italy

M. Scalora

Weapons Sciences Directorate, AMSMI-RD-WS, Development and Engineering Center, U.S. Army Missile Command, Building 7804, Redstone Arsenal, Alabama 35898-5000

M. Bertolotti

Istituto Nazionale Fisícs della Materia, Dipartimento di Energetica, Università di Roma "La Sapienza," Via A. Scarpa, 16, I-00161 Rome, Italy

Received June 8, 1999; revised manuscript received February 7, 2000

A theoretical analysis of the nonlinear quadratic interaction between two monochromatic plane waves at frequencies ω and 2ω in a Fabry–Perot cavity shows that all-optical control of reflectivity and transmissivity of the fundamental beam is possible under suitable conditions. We report all-optical switching of the fundamental beam for cavity lengths that vary from a few micrometers to a few millimeters. Specifically, we show that 100% all-optical switching can occur for a 6-μm cavity when the nonlinear coefficient is not greater than 20 pm/V and the input intensity does not exceed 10 GW/cm^2. Our analytical results are obtained without use of the slowly varying envelope approximation and without resort to the undepleted-pump approximation.
 [S0740-3224(00)00607-X]
OCIS codes: 190.2620, 190.4360.

1. INTRODUCTION

Recently, intensity-dependent phase distortions that arise from quadratic processes in noncentrosymmetric crystals have attracted a great deal of attention. Although nonlinear phase distortions that arise in quadratic processes have been studied since the late 1960's,[1–8] there has been renewed interest in the subject matter, mainly in connection with the search for a practical, ultrafast, low-power, lossless approach to all-optical processing of signals. For more than a decade, beginning during the second half of the 1970's through the late 1980's, degenerate cubic [$\chi^{(3)}$] nonlinear effects have been preferred in all-optical processing schemes [an overview of the nonlinear all-optical devices schemes based on $\chi^{(3)}$ material can be found in Ref. 9]. However, a significant obstacle to the use of these effects has emerged: The implementation of all-optical devices based on cubic nonlinearities that could operate at reasonable power levels is difficult because nonresonant Kerr coefficients are quite small. In a search for alternative schemes, quadratic nonlinear effects were reconsidered after it was realized that nonlinear phase modulation effects also arise in this case that give rise to large nonlinear phase shifts that are promising for use in all-optical devices without the detrimental effects, such as nonlinear absorption and saturation, that appear in Kerr-like nonlinear media.

"The possibility of the use of the effects of nonlinear refraction on the quadratic nonlinearity of crystals for creation of low-threshold ultra-fast apparatus for control of light by light" was highlighted by Belashenkov *et al.* in 1989.[10] Although a number of reports of a phase shift in quadratic processes abound, it was not until 1992 that DeSalvo *et al.*[11] monitored an induced phase change by a $\chi^{(2)}$ process in a KTP crystal by using the Z-scan technique. In the experiment, they clearly demonstrated large nonlinear phase shifts. This experiment paved the way to the experimental investigation in other nonlinear quadratic materials: β-barium borate by means of self-diffraction,[12] potassium niobate,[13] potassium dihydrogen phosphate,[14] organic N-(4-nitrophenyl-L-prolinol,[15] and periodically poled lithium niobate.[16] A theoretical description of nonlinear phase distortions in $\chi^{(2)}$ materials was made by numerical integration of the nonlinear differential equations that describe the propa-

gation of plane waves.[17–19] Analytical studies have been also performed,[20–22] and from an analytical point of the seminal paper of Armstrong *et al.* provided many data.[23] Nonlinear phase distortions that arise from the quadratic interaction have been extensively studied in a great variety of configurations in the framework of all-optical processing of signals [an overview of the nonlinear all-optical devices schemes based on $\chi^{(2)}$ material can be found in Ref. 24].

$\chi^{(2)}$ processes in a cavity configuration have dealt primarily with the problem of optimal intracavity second-harmonic generation[25–27] or with the problem of the generation of squeezed light.[28,29] Within the framework of all-optical signal processing, nonlinear phase distortions induced by $\chi^{(2)}$ processes inside a cavity were numerically studied in Refs. 30 and 31. In particular, a new scheme for highly efficient all-optical switching in a microcavity was studied numerically by Cojocaru *et al.*[32] Although direct numerical integration of the equations of motion without any doubt provides a unique tool for the study of nonlinear phase shifts, we believe that a sound analytical approach can help to put the problem on a more solid theoretical footing. This is what we seek to undertake in this paper. Here we present an analysis devoted to the study of the following case: A beam at frequency ω and a beam of frequency 2ω are incident onto the surface of a Fabry–Perot cavity filled with a nonlinear $\chi^{(2)}$ material. Inside the cavity, the fundamental and second-harmonic fields undergo nonlinear, strong phase-modulation effects that emulate an effective third-order nonlinearity. We show that the characteristic optical response at both fundamental and second-harmonic frequencies can be fully described analytically, provided that the initial relative input phases of the incident fields are locked in a suitable way and that proper boundary conditions are imposed at the input and output cavity mirrors. Exact formulas for the dependence of the reflectivity and the transmissivity at both fundamental and second-harmonic fields are derived. The results suggest the possibility of using this geometry in an all-optical switching device.

From a conceptual point of view, our approach to the problem is similar to that proposed by Berger.[26] However, we do not assume the undepleted-pump or the slowly varying envelope approximation, and we calculate particular nonlinear eigenmodes of the fields inside the cavity for both the fundamental and the second-harmonic fields. Our results clearly suggest the possibility of obtaining 100% all-optical switching even for a cavity with only 6 μm of nonlinear material and whose nonlinear coefficient is approximately 20 pm/V. Input intensities do not exceed 10 GW/cm^2. Generally, we find that threshold input intensities are greatly reduced if one considers longer cavities.

The paper is organized as follows: In Section 2 we discuss the basic equations that govern the quadratic interaction in a cavity and describe the mathematical approach used in deriving first-order nonlinear differential equations for the backward and forward amplitudes. We also discuss the boundary conditions that we impose at the input and output surfaces of the cavity used to arrive at solutions, which we describe in Section 3. In that section we also describe the conditions needed to achieve 100% all-optical switching for different cavity lengths. In Section 4 we discuss a simple example of all-optical switching in a 6-μm cavity.

Our theoretical results are encouraging within the framework of a low-power, lossless approach to all-optical processing of signals.

2. BASIC EQUATIONS AND BOUNDARY CONDITIONS

The interaction of two monochromatic plane waves in a quadratic material is governed by a set of two second-order, coupled nonlinear equations for the complex amplitudes at ω and 2ω:

$$\frac{d^2A_\omega}{dz^2} + k_\omega{}^2A_\omega = -\alpha A_\omega{}^*A_{2\omega},$$

$$\frac{d^2A_{2\omega}}{dz^2} + k_{2\omega}{}^2A_{2\omega} = -2\alpha A_\omega{}^2, \tag{1}$$

where $k_\omega = k_0 n_\omega$ and $k_{2\omega} = 2k_0 n_{2\omega}$; and n_ω and $n_{2\omega}$ are the linear refractive indices of the material at frequencies ω and 2ω, respectively; $k_0 = \omega/c$ (c is the speed of light in vacuum); and $\alpha = 2k_0{}^2 d$ is the nonlinear coupling constant, where d is proportional to the nonlinear susceptibility $\chi^{(2)}$. Typically, d may be several picometers per volt. By means of the one-dimensional Green functions $g(z, z')$

$$g_{j\omega}(z, z') = \frac{\exp(ik_{j\omega}|z - z'|)}{2ik_{j\omega}}, \quad j = 1, 2, \tag{2}$$

we can transform the two differential equations given in Eqs. (1) in two integral equations:

$$A_\omega(z) = -a\int_{-\infty}^{+\infty} g_\omega(z, z')A_\omega{}^*(z')A_{2\omega}(z')dz', \tag{3a}$$

$$A_{2\omega}(z) = -2\alpha\int_{-\infty}^{+\infty} g_{2\omega}(z, z')A_\omega{}^2(z')dz'. \tag{3b}$$

Equations (3) can be rewritten in the simple form

$$A_{j\omega}(z) = A_{+j\omega}(z)\exp(ik_{j\omega}z) + A_{-j\omega}(z)\exp(-ik_{j\omega}z), \quad j = 1, 2, \tag{4}$$

where

$$\begin{aligned} A_{+\omega}(z) = -\frac{\alpha}{2ik_\omega}\int_{-\infty}^{z} \{&A_{+\omega}{}^*(z')A_{+2\omega}(z')\exp[i(k_{2\omega} \\ &- 2k_\omega)z'] \\ &+ A_{-\omega}{}^*(z')A_{+2\omega}(z')\exp(ik_{2\omega}z') \\ &+ A_{+\omega}{}'(z')A_{-2\omega}(z')\exp[-i(k_{2\omega} + k_\omega)z'] \\ &+ A_{-\omega}{}^*(z')A_{-2\omega}(z')\exp(-ik_{2\omega}z')\}dz', \end{aligned} \tag{4a}$$

$$A_{-\omega}(z) = -\frac{\alpha}{2ik_{\omega}}\int_{z}^{-\infty}\{A_{+\omega}^{*}(z')A_{+2\omega}(z')\exp(ik_{2\omega}z') + A_{-\omega}^{*}(z')A_{+2\omega}(z')\exp[i(k_{2\omega}+2k_{\omega})z'] + A_{+\omega}'(z')A_{-2\omega}(z')\exp(-ik_{2\omega}z') + A_{-\omega}^{*}(z')A_{-2\omega}(z')\exp[-i(k_{2\omega}-2k_{\omega})z']\}dz', \quad (4b)$$

$$A_{+2\omega}(z) = -\frac{\alpha}{ik_{2\omega}}\int_{-\infty}^{z}\{A_{+\omega}^{2}(z')\exp[-i(k_{2\omega}-2k_{\omega})z'] + A_{-\omega}^{2}(z')\exp[-i(k_{2\omega}+2k_{\omega})z'] + 2A_{+\omega}(z')A_{-\omega}(z')\exp(-ik_{2\omega}z')\}dz', \quad (4c)$$

$$A_{-2\omega}(z) = -\frac{\alpha}{2ik_{2\omega}}\int_{z}^{-\infty}\{A_{+\omega}^{2}(z')\exp[i(k_{2\omega}+2k_{\omega})z'] + A_{-\omega}^{2}(z')\exp[i(k_{2\omega}-2k_{\omega})z'] + 2A_{+\omega}(z')A_{-\omega}(z')\exp(ik_{2\omega}z')\}dz'. \quad (4d)$$

Note that Eqs. (4a)–(4d) define the forward- and backward-traveling wave amplitudes, and $\exp(ik_{j\omega}z)$ and $\exp(-ik_{j\omega}z)$ in Eqs. (4) are their normal modes. We stress that the form of the solutions given in Eqs. (4) is derived directly from integral equations (3), and it is not an assumed form. We can now reduce the four integral equations for the forward and backward wave amplitudes given in Eqs. (4a)–(4b) to four first-order differential equations by simply taking the derivative of each of Eqs. (4a)–(4b) with respect to the propagation direction z:

$$\frac{dA_{+\omega}}{dz} = -\frac{\alpha}{2ik_{\omega}}\{A_{+\omega}^{*}A_{+2\omega}\exp[i(k_{2\omega}-2k_{\omega})z] + A_{-\omega}^{*}A_{+2\omega}\exp(ik_{2\omega}z) + A_{+\omega}^{*}A_{-2\omega}\exp[-i(k_{2\omega}+2k_{\omega})z] + A_{-\omega}^{*}A_{-2\omega}\exp(-ik_{2\omega}z)\}, \quad (5a)$$

$$\frac{dA_{-\omega}}{dz} = \frac{\alpha}{2ik_{\omega}}\{A_{+\omega}^{*}A_{+2\omega}\exp(ik_{2\omega}z) + A_{-\omega}^{*}A_{+2\omega}\exp[ik_{2\omega}+2k_{\omega})z] + A_{+\omega}^{*}A_{-2\omega}\exp(-ik_{2\omega}z) + A_{-\omega}^{*}A_{-2\omega}\exp[-i(k_{2\omega}-2k_{\omega})z)\}, \quad (5b)$$

$$\frac{dA_{+2\omega}}{dz} = -\frac{\alpha}{ik_{\omega}}\{A_{+\omega}^{2}\exp[-i(k_{2\omega}-2k_{\omega})z] + A_{-\omega}^{2}\exp[-i(k_{2\omega}+2k_{\omega})z] + 2A_{+\omega}A_{-\omega}\exp(-i(k_{2\omega}z)\}, \quad (5c)$$

$$\frac{dA_{-2\omega}}{dz} = \frac{\alpha}{ik_{2\omega}}\{A_{+\omega}^{2}\exp[i(k_{2\omega}+2k_{\omega})z] + A_{-\omega}^{2}\exp[i(k_{2\omega}-2k_{\omega})z] + 2A_{+\omega}A_{-\omega}\exp(ik_{2\omega}z)\}. \quad (5d)$$

Once again, we emphasize the fact that, to obtain the four first-order differential equations given in Eqs. (5), starting from the two second-order Helmholtz equations given in Eqs. (1), we have not assumed the slowly varying envelope approximation. In fact, it can be shown that in general it is not necessary to invoke the slowly varying envelope approximation to simplify the equations of the coupled-wave theory.[33–35] Now we invoke the usual rotating-wave approximation, which consists in neglecting the fast-oscillating components. As a result, it is possible to decouple the forward and backward modes of the interacting fields in Eqs. (5). We obtain the following system of differential equations:

$$\frac{dA_{\pm\omega}}{dz} = \pm i\frac{\alpha}{2k_{\omega}}A_{\pm2\omega}A_{\pm\omega}^{*}\exp(\pm i\Delta kz), \quad (6a)$$

$$\frac{dA_{\pm2\omega}}{dz} = \pm i\frac{\alpha}{k_{2\omega}}A_{\pm\omega}^{2}\exp(\mp i\Delta kz), \quad (6b)$$

where $\Delta k = k_{2\omega} - 2k_{\omega}$ is the usual phase mismatch.

Now we discuss the boundary conditions that must be imposed at the input and output surfaces of the Fabry–Perot cavity. The geometry that we consider is depicted in Fig. 1. Two plane waves, $E_{\omega}^{(i)}$ and $E_{2\omega}^{(i)}$ at frequencies ω and 2ω, respectively, propagating in a linear medium (air, for example), are incident upon the left input mirror of a Fabry–Perot interferometer filled with a thickness L of nonlinear material. The transmission and reflection properties of the input and output linear mirrors can be summarized as follows:

$$r_{kl}^{(j\omega)} = |r_{kl}^{(j\omega)}|\exp[i\varphi_{rkl}^{(j\omega)}], \quad (7a)$$

$$t_{kl}^{(j\omega)} = |t_{kl}^{(j\omega)}|\exp[i\varphi_{tkl}^{(j\omega)}],$$

$$j = 1, 2, \qquad k, l = 1, 2, 3, \qquad k \neq 1, \quad (7b)$$

where the superscript $j\omega$ indicates the mirror response at the fundamental or second-harmonic frequency and the subscript kl refers to light incident from region kth onto region lth, as shown in Fig. 1. For simplicity, we con-

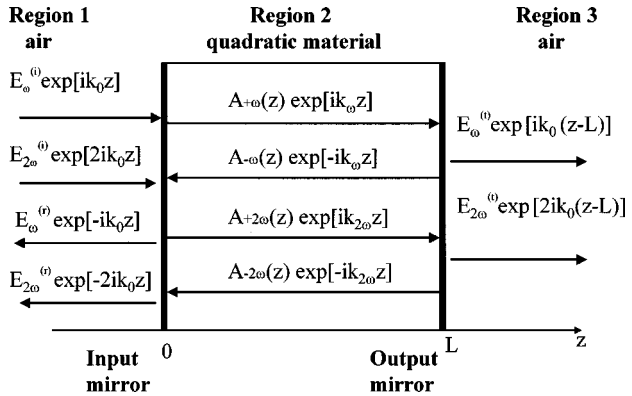

Fig. 1. Schematic representation of the geometry that we analyze. Two plane waves, $E_{\omega}^{(i)}$ and $E_{2\omega}^{(i)}$, at frequencies ω and 2ω propagating in a linear medium (air) are incident at the input mirror of a Fabry–Perot interferometer filled with a thickness L of quadratic material. $E_{\omega}^{(r)}$ and $E_{2\omega}^{(r)}$ are the reflected components; $E_{\omega}^{(t)}$ and $E_{2\omega}^{(t)}$ are the transmitted components.

sider nonabsorbing mirrors. As a result, their reflection and transmission coefficients satisfy the following relations:

$$|r_{12}{}^{j\omega}|^2 + n_{j\omega}|t_{12}{}^{j\omega}|^2 = 1, \tag{8a}$$

$$|r_{32}{}^{j\omega}|^2 + n_{j\omega}|t_{32}{}^{j\omega}|^2 = 1, \tag{8b}$$

$$|r_{21}{}^{j\omega}|^2 + \frac{1}{n_{j\omega}}|t_{21}{}^{j\omega}|^2 = 1, \tag{8c}$$

$$|r_{23}{}^{j\omega}|^2 + \frac{1}{n_{j\omega}}|t_{23}{}^{j\omega}|^2 = 1, \quad j = 1, 2 \tag{8d}$$

where $n_{j\omega}$ and $(l/n_{j\omega})$ are factors that take into account the difference in phase velocity in regions 1 and 3 (in air, $n = 1$) and the phase velocity in region 2 at the fundamental and second-harmonic frequencies. Refer to Fig. 1; at the input surface ($z = 0$) the amplitudes of the incident and the reflected waves are linked to the nonlinear backward and forward cavity modes by the following reltions:[36]

$$A_{+j\omega}(0) = t_{12}{}^{(j\omega)}E_{j\omega}{}^{(i)} + r_{21}{}^{(j\omega)}A_{-j\omega}(0), \tag{9a}$$

$$E_{j\omega}{}^{(r)} = r_{12}{}^{(j\omega)}E_{j\omega}{}^{(i)} + t_{21}{}^{(j\omega)}A_{-j\omega}(0), \quad j = 1, 2. \tag{9b}$$

At the output surface ($z = L$) the link between the nonlinear cavity modes and the amplitudes of the transmitted waves is given by the following relations:

$$E_{j\omega}{}^{(t)} = t_{23}{}^{(j\omega)}A_{+j\omega}(L)\exp(ik_{j\omega}L), \tag{9c}$$

$$A_{-j\omega}(L) = r_{23}{}^{(j\omega)}A_{+j\omega}(L)\exp(2ik_{j\omega}L), \quad j = 1, 2. \tag{9d}$$

We note that, if one considers the linear eigenmodes of the cavity without taking into account the nonlinear interaction in the quadratic material [i.e., $dA_{\pm j\omega}/dz = 0$ and hence $A_{\pm j\omega}(0) = A_{\pm j\omega}(L) = C_{\pm j\omega}$ for $j = 1, 2$], then

$$A_{j\omega}(z) = C_{+j\omega}\exp(ik_{j\omega}z) + C_{-j\omega}\exp(-ik_{j\omega}z), \quad j = 1, 2. \tag{10}$$

From the boundary conditions given in Eqs. (9), it follows, after some algebra, that

$$T_{j\omega}{}^{(\mathrm{linear})} = \frac{t_{12}{}^{(j\omega)}t_{23}{}^{(j\omega)}\exp)(ik_{j\omega}L)}{1 + r_{21}{}^{(j\omega)}r_{23}{}^{(j\omega)}\exp(2ik_{j\omega}L)}, \quad j = 1, 2. \tag{11}$$

where $T_{j\omega}{}^{(\mathrm{linear})} = E_{j\omega}{}^{(t)}/E_{j\omega}{}^{(i)}$. The expression in Eq. (11) is just the standard transmission function of the Fabry–Perot interferometer.[36] We adopt the superscript "linear" to distinguish the above expression from the transmissivity in the nonlinear regime, which we calculate in Section 3.

3. NONLINEAR EIGENMODES AND ANALYTICAL EXPRESSIONS FOR THE NONLINEAR TRANSMISSIVITY FUNCTION

Equations (6) above have been extensively studied in a bulk medium. Their general solutions in terms of elliptic integrals first appeared in the pioneering paper of Armstrong *et al.*[23] Even if the analytical solutions of Eqs. (6) are well known in terms of elliptic integrals, it is nevertheless a formidable task to match the analytical solutions with the boundary conditions given by Eqs. (9) to calculate the reflected and transmitted fields $E_{j\omega}{}^{(r)}$ and $E_{j\omega}{}^{(t)}$ at both the fundamental and the second-harmonic frequencies. General expressions for the transmitted and reflected fields are not available because the solution of Eqs. (6) must be expressed in terms of eight parameters (i.e., amplitude and phase of the fundamental and the second-harmonic fields for both the backward and the forward modes at the input surface, just inside the quadratic material at $z = 0$), which are embedded within the elliptic integrals in a nontrivial manner. Moreover, these solutions are linked to the input, reflected, and transmitted fields by the boundary conditions in Eqs. (9) also in a nontrivial manner.

We thus look for particular solutions that make possible the derivation of analytical expressions for the transmissivity and reflectivity functions of the structure. We investigate the case in which the nonlinear interaction inside the quadratic material takes place under the phase-matching condition $\Delta k = k_{2\omega} - 2k_{\omega} = 0$. Under these circumstances the system of Eqs. (6) admits of eigenmodes with the property of no energy exchange[37] that can easily be matched with the boundary conditions given by Eqs. (9). It is then possible to write analytical expressions for the transmissivity and reflectivity functions for both the fundamental and the second-harmonic fields. We consider the following expressions for the amplitudes of the backward- and forward-traveling waves inside the cavity:

$$A_{\pm\omega}(z) = (-i)^{m_\pm}\sqrt{2}|A_{\pm 2\omega}(0)|\exp\left[\pm i(-i)^{m_\pm}\Gamma|A_{\pm 2\omega}(0)|z + i\frac{\phi_{\pm 2\omega}(0)}{2}\right], \tag{12a}$$

$$A_{\pm 2\omega}(z) = |A_{\pm 2\omega}(0)|\exp[\pm i2(-1)^{m_\pm}\Gamma|A_{\pm 2\omega}(0)|z + i\phi_{\pm 2\omega}(0)], \tag{12b}$$

where m_+ and m_- can be any integer number and $\Gamma = \omega d/n_{\omega}c$. One can easily verify that the above expressions for the amplitude of the forward- and backward-traveling waves are solutions of the system of differential equations (6) when $\Delta k = 0$ by simple direct substitution. We note that in Eqs. (12) the amplitudes and phases of the nonlinear eigenmodes of the fundamental and the second harmonic at $z = 0$ are linked by

$$|A_{\pm\omega}(0)| = \sqrt{2}|A_{\pm 2\omega}(0)|, \tag{13a}$$

$$\varphi_{\pm 2\omega}(0) - 2\varphi_{\pm\omega}(0) = m_\pm\pi. \tag{13b}$$

We shall discuss these conditions below. For the time being, we note that these solutions do not show an amplitude modulation; rather, they display linearly growing phase distortions that depend on the field amplitude inside the quadratic material and on the magnitude of coupling constant d. Matching the solutions given by Eqs. (12a) and (12b) with the boundary conditions given by Eqs. (9a)–(9d), and after some tedious algebraic manipulations, we obtain the expressions for the transmission

and reflection functions at the fundamental and second-harmonic frequencies. Writing the transmission functions in amplitude and phase representation $\{T_{j\omega} = |T_{j\omega}|\exp[i\varphi_T^{(j\omega)}]\}$, we obtain the following expressions for the square modulus of the transmissivity functions (transmittance):

$$|T_\omega|^2 = \frac{|t_{12}^{(\omega)}|^2|t_{23}^{(\omega)}|^2}{[1 - |r_{21}^{(\omega)}||r_{23}^{(\omega)}|]^2 + 4|r_{21}^{(\omega)}||r_{23}^{(\omega)}|\sin^2\left\{k_\omega L + \frac{\tilde{\Gamma}L\sqrt{I_{2\omega}^{(t)}}}{2|t_{23}^{(2\omega)}|}[(-1)^{m_+} + (-1)^{m_-}|r_{23}^{(2\omega)}|] + \frac{\varphi_{r23}^{(\omega)} + \varphi_{r21}^{(\omega)}}{2}\right\}}, \tag{14a}$$

$$|T_{2\omega}|^2 = \frac{|t_{12}^{(2\omega)}|^2|t_{23}^{(2\omega)}|^2}{[1 - |r_{21}^{(2\omega)}||r_{23}^{(2\omega)}|]^2 + 4|r_{21}^{(2\omega)}\|r_{23}^{(2\omega)}|\sin^2\left\{2k_\omega L + \frac{\tilde{\Gamma}L\sqrt{I_{2\omega}^{(t)}}}{|t_{23}^{(2\omega)}|}[(-1)^{m_+} + (-1)^{m_-}|r_{23}^{(2\omega)}|] + \frac{\varphi_{r23}^{(2\omega)} + \varphi_{r21}^{(2\omega)}}{2}\right\}} \tag{14b}$$

and the following expressions for the phases:

$$\varphi_T^{(\omega)} = \varphi_{t12}^{(\omega)} + \varphi_{t23}^{(\omega)} + k_\omega L + (-1)^{m_+}\frac{\tilde{\Gamma}L\sqrt{I_{2\omega}^{(t)}}}{|t_{23}^{(2\omega)}|} - \arctan\left[\frac{|r_{21}^{(\omega)}||r_{23}^{(\omega)}|\sin\left\{\varphi_{r21}^{(\omega)} + \varphi_{r23}^{(\omega)} + 2k_\omega L + \frac{\tilde{\Gamma}L\sqrt{I_{2\omega}^{(t)}}}{|t_{23}^{(2\omega)}|}[(-1)^{m_+} + (-1)^{m_-}|r_{23}^{(2\omega)}|]\right\}}{|r_{21}^{(\omega)}||r_{23}^{(\omega)}|\cos\left\{\varphi_{r21}^{(\omega)} + \varphi_{r23}^{(\omega)} + 2k_\omega L + \frac{\tilde{\Gamma}L\sqrt{I_{2\omega}^{(t)}}}{|t_{23}^{(2\omega)}|}[(-1)^{m_+} + (-1)^{m_-}|r_{23}^{(2\omega)}|]\right\} - 1}\right], \tag{14c}$$

$$\varphi_T^{(2\omega)} = \varphi_{t12}^{(2\omega)} + \varphi_{t23}^{(2\omega)} + 2k_\omega L + (-1)^{m_+}\frac{2\tilde{\Gamma}L\sqrt{I_{2\omega}^{(t)}}}{|t_{23}^{(2\omega)}|} - \arctan\left[\frac{|r_{21}^{(2\omega)}||r_{23}^{(2\omega)}|\sin\left\{\varphi_{r21}^{(2\omega)} + \varphi_{r23}^{(2\omega)} + 4k_\omega L + \frac{2\tilde{\Gamma}L\sqrt{I_{2\omega}^{(t)}}}{|t_{23}^{(2\omega)}|}[(-1)^{m_+} + (-1)^{m_-}|r_{23}^{(2\omega)}|]\right\}}{|r_{21}^{(2\omega)}||r_{23}^{(2\omega)}|\cos\left\{\varphi_{r21}^{(2\omega)} + \varphi_{r23}^{(2\omega)} + 4k_\omega L + \frac{\tilde{\Gamma}L\sqrt{I_{2\omega}^{(t)}}}{|t_{23}^{(2\omega)}|}[(-1)^{m_+} + (-1)^{m_-}|r_{23}^{(2\omega)}|]\right\} - 1}\right], \tag{14d}$$

where $I_{2\omega}^{(t)}$ is the transmitted intensity of the second-harmonic field, $\tilde{\Gamma} = \Gamma[2/(\epsilon_0 c)]^{1/2}$, and ϵ_0 is the vacuum dielectric permittivity. We note that in our model the transmitted intensity of the second-harmonic field $I_{2\omega}^{(t)}$ is a free parameter that can be arbitrarily chosen. It determines the transmittance for both the fundamental and the second-harmonic fields: it plays the role of a control parameter. Equations (13a) and (13b) lead to well-defined constraints on the intensity and phase of the fields incident upon the input surface of the Fabry–Perot interferometer and upon the reflectivity of the output mirror. The input intensity of the fundamental field $I_\omega^{(i)}$ cannot be chosen as a free parameter. It is related to the transmitted intensity of the second-harmonic field $I_{2\omega}^{(t)}$ by the following expression:

$$I_\omega^{(i)} = 2\frac{|t_{23}^{(\omega)}|^2}{|t_{23}^{(2\omega)}|^2}\frac{I_{2\omega}^{(t)}}{|T_\omega|^2}. \tag{15a}$$

The input phases of the fundamental and the second-harmonic fields are then related through the following expression:

$$\varphi_{2\omega}^{(i)} - 2\varphi_\omega^{(t)} = m_+\pi + 2\varphi_T^{(\omega)} - \varphi_T^{(2\omega)} + \varphi_{t23}^{(2\omega)} - 2\varphi_{t23}^{(\omega)}. \tag{15b}$$

Moreover, the reflectivity $r_{23}^{(j\omega)}$ of the output mirror at the fundamental and second-harmonic frequencies must satisfy the following relations:

$$|r_{23}^{(2\omega)}| = |r_{23}^{(\omega)}|, \tag{16a}$$

$$\varphi_{r23}^{(2\omega)} - 2\varphi_{r23}^{(\omega)} = \pi(m_- - m_+). \tag{16b}$$

We shall explore these constraints and their physical implications for the output mirrors below. The expressions for the transmittance that we derived in Eqs. (14a) and (14b) differ from the standard linear transmittance functions of a Fabry–Perot cavity because they are shifted by an intensity-dependent phase factor, namely,

$$\delta = j\frac{\tilde{\Gamma}L\sqrt{I_{2\omega}^{(t)}}}{2|t_{23}^{(2\omega)}|}[(-1)^{m_+} + |r_{23}^{(2\omega)}|(-1)^{m_-}], \qquad j = 1, 2. \tag{17}$$

When $\delta = \pi/2$, the cavity switches from maximum transmission to a reflection minimum. This situation reverses for every $\pm\pi/2$ of accumulated phase. We therefore obtain the switching threshold intensity necessary for all-optical switching by setting $\delta = \pi/2$. We find that

$$I_{2\omega}^{(t)\mathrm{thr}\,j\omega} = \frac{\pi^2 |t_{23}^{(2\omega)}|^2}{j\tilde{\Gamma}^2 L^2 [(-1)^{m_+} + |r_{23}^{(2\omega)}|(-1)^{m_-}]^2}, \quad j = 1, 2, \tag{18}$$

where the superscript "thr $j\omega$" indicates the threshold value of the transmitted second-harmonic intensity that will switch the cavity from an on to an off state, or vice versa, at the fundamental or second-harmonic frequency. By means of condition (15a), which links the second-harmonic transmitted intensity to the fundamental input intensity, we obtain the corresponding threshold value for the fundamental input intensity:

$$I_{\omega}^{(i)\mathrm{thr}\,j\omega} = \frac{2\pi^2 |t_{23}^{(\omega)}|^2}{j\tilde{\Gamma}^2 L^2 |T_{\omega}|^2 [(-1)^{m_+} + |r_{23}^{(2\omega)}|(-1)^{m_-}]^2}, \quad j = 1, 2. \tag{19}$$

We point out that threshold intensities for all-optical switching are reduced significantly if the transmittance of the output mirror is small at both the fundamental and the second-harmonic frequencies, as Eqs. (18) and (19) suggest. The use of mirrors characterized by low transmittance values is required for a high-finesse Fabry–Perot cavity to be achieved. As a consequence, the efficiency of the nonlinear interaction is also determined and enhanced by the geometrical properties of the cavity.

Output mirrors with high reflectivity and no absorption are available in the form of multilayer dielectric stacks. Recently these periodic dielectric structures, usually referred to as photonic bandgap crystals, have been the subject of intense theoretical and experimental investigations,[38–43] also within the context of efficient second-harmonic generation.[44,45] One of the remarkable properties of photonic crystals is the existence of several spectral passbands and bandgaps at which the value of transmittance can be extremely low (typically the transmittance in the gap can be as low as 10^{-4}; therefore the reflectance approaches values close to unity). In our case we need an output mirror that satisfies the condition given by Eqs. (16): It must also have low transmittance at both the fundamental and the second-harmonic fields. We also note that, from Eqs. (18) and (19), the threshold input intensities are minimized if $m_+ = m_-$. Going back to Eqs. (16) and taking the above considerations into account, we obtain that optimum conditions at the output mirror can be realized if the reflectance is taken to be

$$|r_{23}^{(2\omega)}| = |r_{23}^{\omega}| \cong (1 - 10^{-4}) \tag{20a}$$

and the phases are related by

$$\varphi_{r23}^{(2\omega)} = 2\varphi_{r23}^{(\omega)}. \tag{20b}$$

The condition imposed by relation (20a) and Eq. (20b) can easily be fulfilled by use of a multilayer stack composed of 10 alternating layers of SiO_2 and TiO_2 materials, such that SiO_2 is taken to be a quarter-wave layer and TiO_2 is taken to be a half-wave layer with respect to the reference wavelength. The resultant band structure, shown in Fig. 2 in scaled units, contains a second-order reflectivity region near $\Omega = \omega/\omega_0 = 1.35$, which is separated from the first-order reflectivity region by a factor of 2. That is, if we choose the fundamental field near the scaled $\Omega = 0.675$, the mirror will be highly reflective at both the fundamental and the second-harmonic frequencies; this satisfies relation (20a). To satisfy Eq. (20b) we calculate the phase properties of the mirror on reflection, which we also depict in Fig. 2 by the dotted curve. The figure clearly suggests that the phase relationship of Eq. (20b) that we impose is easily satisfied by our proposed output mirror. We note that the materials that we have selected are not unique. The same phase characteristics can be obtained with semiconductor or dielectric structures, as long as the quarter–half-wavelength thickness requirement is approximately satisfied.

4. EXAMPLE OF ALL-OPTICAL SWITCHING

In this section we discuss a simple example that will illustrate all-optical switching of the fundamental field at moderate input intensities. We consider a Fabry–Perot cavity filled with 6.1574 μm of a nonlinear ideal material, with its nonlinear coefficient $d = 20$ pm/V. We assume that the material is phase matched at $\lambda_\omega = 1.064$ μm and $\lambda_{2\omega} = 532$ nm, with a refractive index $n_\omega = n_{2\omega} = 2.16$. The reflection and transmission coefficients of the mirrors are chosen such that

$$|t_{12}^{(\omega)}| = |t_{12}^{(2\omega)}| = 1.851 \times 10^{-2},$$
$$|r_{21}^{(\omega)}| = |r_{21}^{2(\omega)}| = 9.996 \times 10^{-1},$$
$$|t_{23}^{(\omega)}| = |t_{23}^{(2\omega)}| = 3.998 \times 10^{-2},$$
$$|r_{23}^{(\omega)}| = |r_{23}^{(2\omega)}| = 9.996 \times 10^{-1},$$

in agreement with the relations given by Eqs. (8) and the condition imposed on the output mirror by relation (20a). The resultant high-Q Fabry–Perot cavity is characterized by transmission resonance bandwidths of ~0.1 nm for the

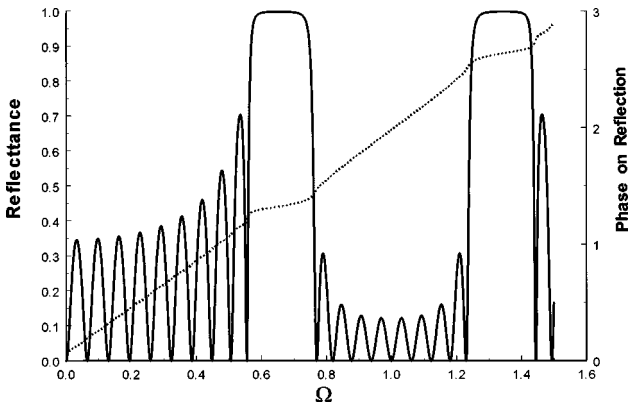

Fig. 2. Band structure (solid curve) of a dielectric mirror composed of 10 alternating layers of SiO_2 and TiO_2 materials, such that SiO_2 is taken to be a quarter-wave layer and TiO_2 is taken to be a half-wave layer with respect to a reference wavelength. $\Omega = \omega/\omega_0$, where ω_0 corresponds to a reference wavelength of 1 μm. Dotted curve, the phase of the field (in units of π) on reflection from the dielectric stack.

fundamental field and 0.06 nm for the second-harmonic field. The transmittance in the linear regime at both the fundamental and the second harmonic as a function of cavity length L is shown in Fig. 3. Because the values of $\varphi_{r12}^{(j\omega)}$, $\varphi_{t12}^{(j\omega)}$, and $\varphi_{t23}^{(j\omega)}$ are not subject to any constraints, we choose them such that for the chosen cavity length a transmission peak is obtained for the second-harmonic field, whereas the fundamental field is completely reflected in the linear regime. We show these features in Figs. 3 and 4. Thus the fundamental field can switch from a total-reflection, off state to a total-transmission, on state, provided that the second-harmonic intensity is chosen to be above the threshold given by Eq. (18), which for $m_+ = m_-$ and $j = l$ becomes

$$I_{2\omega}^{(t)\mathrm{thr}\,\omega} = \frac{\pi^2 |t_{23}^{(2\omega)}|^2}{\tilde{\Gamma}^2 L^2 [1 + |r_{23}^{(2\omega)}|]^2}. \tag{21}$$

In our example, this corresponds to a threshold intensity of $I_{2\omega}^{(t)\mathrm{thr}\,\omega} \cong 4.6\,\mathrm{GW/cm^2}$. This value corresponds to a nonlinear phase shift of $\pi/2$, and it causes the fundamental field to switch from an off to an on state; we show this in Fig. 5. At the same time, the phase shift suffered by the second-harmonic field is π. Thus the second-harmonic field remains at a transmission maximum. Under these circumstances, input and output values of the second-harmonic field are identical, i.e.,

$$I_{2\omega}^{(i)\mathrm{thr}\,\omega} = I_{2\omega}^{(t)\mathrm{thr}\,\omega} \cong 4.6\,\mathrm{GW/cm^2}. \tag{22}$$

The corresponding threshold value for the fundamental input intensity is given by Eq. (19), which for $m_+ = m_-$, $j = l$, and $|T_\omega|^2 = 1$ becomes

$$I_{\omega}^{(i)\mathrm{thr}\,\omega} = \frac{2\pi^2 |t_{23}^{(\omega)}|^2}{\tilde{\Gamma}^2 L^2 [1 + |r_{23}^{(2\omega)}|]^2}. \tag{23}$$

This corresponds to $I_{\omega}^{(i)\mathrm{thr}\,\omega} \cong 9.2\,\mathrm{GW/cm^2}$. All that remains to be specified is the link between the input phases of the fields, as given by Eq. (15b). Taking $m_+ = m_- = m$, and using Eqs. (14c) and (14d) calculated in a peak of transmission for both the fundamental and the second harmonic, we have

$$\varphi_{2\omega}^{(i)} - 2\varphi_{\omega}^{(i)} = m\pi + 2\varphi_{t12}^{(\omega)} - \varphi_{t12}^{(2\omega)}. \tag{24}$$

In the example, we have shown that 100% all-optical switching is possible for a cavity that contains approximately 6 μm of nonlinear material, which in this case corresponds to an optical path of approximately three wavelengths. We note that we have chosen a nonlinear coefficient $d = 20\,\mathrm{pm/V}$ and that our input intensity is approximately 10 $\mathrm{GW/cm^2}$. We also point out that threshold input intensities satisfy the following scaling laws:

$$I_{2\omega}^{(i)\mathrm{thr}\,\omega} \approx \frac{1}{L^2}, \qquad I_{\omega}^{(i)\mathrm{thr}\,\omega} \approx \frac{1}{L^2}. \tag{25}$$

Therefore the input intensities can be significantly reduced if one considers longer cavity lengths. For a 600-μm cavity, for example, and a nonlinear coefficient $d = 20\,\mathrm{pm/V}$, all-optical switching of the fundamental field can occur with intensities of the order of 1 $\mathrm{MW/cm^2}$.

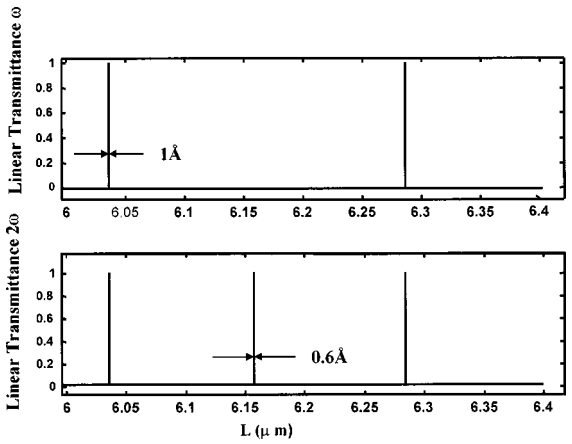

Fig. 3. Transmittance versus L, the length of the nonlinear cavity, in the linear regime for both the fundamental and the second-harmonic fields. The transmission peaks have widths of (~0.1 nm) 1 Å for the fundamental and ~0.6 Å (~0.06 nm) for the second harmonic.

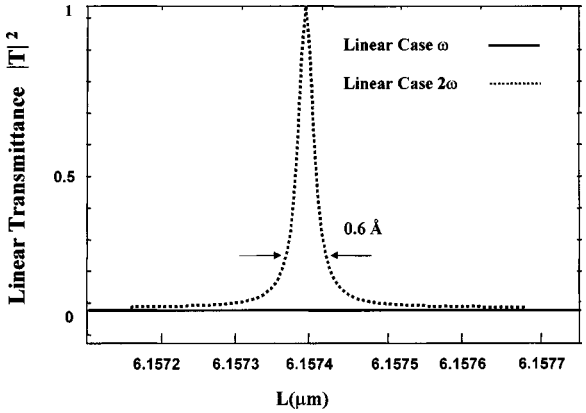

Fig. 4. Linear transmittance of the fundamental (continuous line) and the second-harmonic (dotted curve) fields about a length L of 6.1574 μm of nonlinear material. This corresponds to a peak of transmission for the second-harmonic field and to a reflection maximum for the fundamental field.

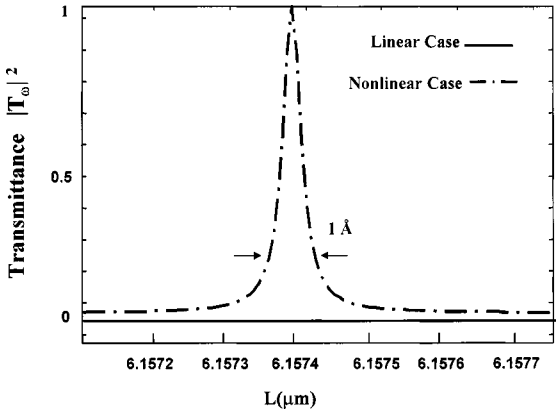

Fig. 5. Transmittance for the fundamental beam in the linear regime and in the nonlinear regime about a length L of 6.1574 μm of nonlinear material. The fundamental field switches from total reflection in the linear regime to total transmission in the nonlinear regime for an input intensity of 9.2 $\mathrm{GW/cm^2}$ for the fundamental field and 4.6 $\mathrm{GW/cm^2}$ for the second-harmonic field. 100% all-optical switching for the fundamental beam is obtained.

In the example we refer to an ideal lossless material. In reality, one has to take into account optical losses of the nonlinear material that fills the cavity, in particular when cavity length approaches the millimeter range. For simplicity, however, we do not include absorption in our model. Although its inclusion would most likely lead to an increase of the threshold intensities, its neglect will not affect the qualitative results that we present. However, the choice of cavity length must be guided by the particular application that one seeks. For example, this effect could be exploited in combination with optical fibers and waveguides in an integrated circuit environment. In that case, short picosecond pulses require transmission resonance bandwidths that may exceed 1 nm, and cavities filled with longer lengths of nonlinear material may provide a better approach than the high-finesse cavities that we have discussed.

5. CONCLUSIONS

In summary, we have explored the nonlinear intensity-dependent phase distortions that arise from quadratic processes in a cavity configuration. The theoretical analysis presented here shows that the nonlinear phase shift can be enhanced in a cavity by several orders of magnitude with respect to free propagation in bulk, quadratic materials. The characteristic optical responses at both fundamental and second-harmonic frequencies, as well as their dependence on the physical parameters of the resonator, have been fully analytically described. All-optical switching has been analytically demonstrated for a cavity with high finesse that contains only 6 μm of nonlinear material and has a nonlinear coefficient of approximately 20 pm/V, and for input intensity not exceeding 10 GW/cm^2. Our results show that it may be possible to implement more-efficient all-optical devices with respect to more-traditional all-optical schemes based on free propagation in bulk, quadratic materials.

ACKNOWLEDGMENTS

We thank Mark J. Bloemer for interesting discussions on the subject. This study has been partially funded by the Esprit-Open project of the European Community. G. D'Aguanno thanks the European Research Office for partial support of this effort.

G. D'Aguanno's e-mail address is daguanno@axrma.uniroma1.it; that of C. Sibilia is sibilia@axrma.uniroma1.it.

REFERENCES

1. L. A. Ostrovskij, "Self-action of light in crystals," JETP Lett. **5**, 272–275 (1967).
2. J. P. Coffinet and F. De Martini, "Coherent excitation of polaritons in gallium phosphide," Phys. Rev. Lett. **22**, 60–63 (1969).
3. T. K. Gustafson, J. P. E. Taran, P. L. Kelley, and R. Y. Chiao, "Self-modulation of picosecond pulses in electro-optics crystals," Opt. Commun. **2**, 17–21 (1970).
4. E. Yablonovitch, C. Flytzanis, and N. Bloembergen, "Anisotropic interference of three-wave and double-two wave frequency mixing in GaAs," Phys. Rev. Lett. **29**, 865–868 (1972).
5. J. M. R. Thomas and J. P. E. Taran, "Pulse distortion in mismatched second harmonic generation," Opt. Commun. **4**, 329–334 (1972).
6. D. N. Klyshko and B. F. Polkovnikov, "Phase modulation and self-modulation of light in three-photon processes," Sov. J. Quantum Electron. **3**, 324–326 (1974).
7. S. A. Akhmanov, A. N. Dubovik, S. M. Saltiel, I. V. Tomov, and V. G. Tunkin, "Nonlinear optical effects of fourth order in the field in a lithium formiate crystal," JETP Lett. **20**, 117–118 (1974).
8. J. M. Jarborough and O. Amman, "Simultaneous optical parametric oscillation, second harmonic generation and difference-frequency generation," Appl. Phys. Lett. **18**, 145–147 (1971).
9. G. I. Stegeman and P. L. Wa, in *Nonlinear Optical Materials and Devices for Applications in Information Technology* (Kluwer Academic, Dordrecht, The Netherlands, 1995), pp. 285–317.
10. N. R. Belashenkov, S. V. Gagarskij, and M. V. Inochkin, "Nonlinear refraction of light on second harmonic generation," Opt. Spectrosc. (USSR) **66**, 806–808 (1989).
11. R. DeSalvo, D. J. Hagan, M. Sheik-Bahae, G. I. Stegeman, E. W. Van Stryland, and H. Vanherzeele, "Self-focusing and self-defocusing by cascaded second-order effects in KTP," Opt. Lett. **17**, 28–30 (1992).
12. R. Danielius, P. Di Trapani, A. Dubietis, A. Piskarskas, D. Podenas, and G. P. Banfi, "Self-diffraction through cascaded second-order frequency-mixing effects in β-barium borate," Opt. Lett. **18**, 574–576 (1993).
13. Z. Y. Ou, "Observation of nonlinear phase shift in cw harmonic generation," Opt. Commun. **124**, 430–437 (1995).
14. E. Fazio, C. Sibilia, F. Senesi, and M. Bertolotti, "All-optical switching during quasi-collinear second-harmonic generation," Opt. Commun. **127**, 62–68 (1996).
15. Z. Wang, D. J. Hagan, E. W. Van Stryland, J. Zyss, P. Vidakovic, and W. E. Toruellas, "Cascaded second-order effects in *N*-(4-nitrophenyl)-L-prolinol, in a molecular single crystal," J. Opt. Soc. Am. B **14**, 76–86 (1997).
16. P. Vidakovic, D. J. Lovering, J. A. Levenson, J. Webjorn, and P. St. J. Russell, "Large nonlinear phase shift owing to cascaded $\chi^{(2)}$ in quasi-phase matched bulk $LiNbO_3$," Opt. Lett. **22**, 277–279 (1997).
17. G. I. Stegeman, M. Sheik-Bahae, E. W. Van Stryland, and G. Assanto, "Large nonlinear phase shifts in second-order nonlinear optical processes," Opt. Lett. **18**, 13–15 (1993).
18. A. L. Belostotsky, A. S. Leonov, and A. V. Maleshko, "Nonlinear phase change in a type II second-harmonic generation under exact phase-matched conditions," Opt. Lett. **19**, 856–858 (1994).
19. A. Re, C. Sibilia, E. Fazio, and M. Bertolotti, "Field dependent effects in a quadratic nonlinear medium," J. Mod. Opt. **42**, 823–839 (1995).
20. A. Kobyakov and F. Lederer, "Cascading of quadratic nonlinearities: an analytical study," Phys. Rev. A **54**, 3455–3471 (1996).
21. G. D'Aguanno, C. Sibilia, E. Fazio, and M. Bertolotti, "Three-wave mixing in a quadratic material under perfect phase-matching," Opt. Commun. **142**, 75–78 (1997).
22. G. D'Aguanno, C. Sibilia, E. Fazio, E. Ferrari, and M. Bertolotti, "Field phase modulation and input phase and intensity dependence in a nonlinear second-order interaction," J. Mod. Opt. **45**, 1049–1066 (1998).
23. J. A. Armstrong, N. Bloembergen, J. Ducuing, and P. S. Pershan, "Interactions between light waves in a nonlinear dielectric," Phys. Rev. **127**, 1918–1939 (1962).
24. G. Assanto, "Quadratic cascading: effects and applications," in *Beam Shaping and Control with Nonlinear Optics*, F. Kajzar and R. Reinisch, eds. (Plenum, New York, 1998), pp. 341–374.
25. R. L. Byer and A. Piskarskas, eds., Feature on optical parametric oscillation and amplification, J. Opt. Soc. Am. B **10**, 1656–1791; 2148–2243 (1993).

26. V. Berger, "Second-harmonic generation in monolithic cavities," J. Opt. Soc. Am. B **14**, 1351–1360 (1997).
27. C. Simonneu, J. P. Debray, J. C. Harmand, P. Vidakovic, D. J. Lovering, and J. A. Levenson, "Second harmonic generation in a doubly resonant semiconductor microcavity," Opt. Lett. **23**, 1775–1777 (1997).
28. L. A. Lugiato, G. Strini, and F. De Martini, "Squeezed states in second-harmonic generation," Opt. Lett. **8**, 256–258 (1983).
29. R. Paschotta, M. Collet, P. Kurz, K. Fiedler, H. A. Bachor, and J. Mlynek, "Bright squeezed light from a singly resonant frequency doubler," Phys. Rev. Lett. **72**, 3807–3810 (1994).
30. R. Reinisch, E. Popov, and M. Nevière, "Second harmonic generation-induced optical bistability in prism or grating couplers," Opt. Lett. **20**, 854–856 (1995); R. Reinisch, M. Nevière, and E. Popov, "Phase-matched guided wave optical bistability in $\chi^{(2)}$ optical resonators," Opt. Lett. **20**, 2472–2474 (1995).
31. L. Caleo, C. Sibilia, P. Masciulli, and M. Bertolotti, "Nonlinear optical filter based on cascading second order effect," J. Opt. Soc. Am. B **14**, 2315–2324 (1997); C. Sibilia, A. Re, E. Fazio, and M. Bertolotti, "Cascading effect on second-harmonic generation in a ring cavity," J. Opt. Soc. Am. B **13**, 1151–1159 (1996).
32. C. Cojocaru, J. Martorell, R. Vilaseca, E. Fazio, and J. Trull, "Active reflection via phase-insensitive quadratic nonlinear interaction within a microcavity," Appl. Phys. Lett. **74**, 504–506 (1999).
33. J. E. Sipe and G. I. Stegeman, "Comparison of normal mode and total field analysis techniques in planar integrated optics," J. Opt. Soc. Am. **69**, 1676–1683 (1979).
34. B. Crosignani, P. Di Porto, and A. Yariv, "Coupled-mode theory and slowly-varying approximation in guided-wave optics," Opt. Commun. **78**, 237–239 (1990).
35. D. G. Hall, "A comment on the coupled-mode equations used in guided-wave optics," Opt. Commun. **82**, 453–455 (1991).
36. P. Yeh, *Optical Waves in Layered Media* (Wiley, New York, 1988), pp. 87–88.
37. A. E. Kaplan, "Eigenmodes of $\chi^{(2)}$ wave mixings: cross-induced second-order nonlinear refraction," Opt. Lett. **18**, 1223–1225 (1993).
38. E. Yablonovitch, "Inhibited spontaneous emission in solid state physics and electronics," Phys. Rev. Lett. **58**, 2059–2062 (1987).
39. S. John, "Strong localization of photons in certain disordered dielectric superlattices," Phys. Rev. Lett. **58**, 2486–2489 (1987).
40. M. Scalora, R. J. Flynn, S. B. Reinhardt, R. L. Fork, M. J. Bloemer, M. D. Tocci, C. M. Bowden, H. S. Ledbetter, J. M. Bendickson, J. P. Dowling, and R. P. Leavitt, "Ultrashort pulse propagation at the photonic band edge: large tunable group delay with minimal distortion and loss," Phys. Rev. E **54**, 1078–1081 (1996).
41. J. M. Bendickson, J. P. Dowling, and M. Scalora, "Analytic expression for the electromagnetic mode density in finite, one-dimensional, photonic band-gap structures," Phys. Rev. E **53**, 4107–4121 (1996).
42. M. Scalora, M. J. Bloemer, A. S. Pethel, J. P. Dowling, C. M. Bowden, and A. S. Manka, "Transparent metallo-dielectric, one-dimensional, photonic band-gap structures," J. Appl. Phys. **83**, 2377–2382 (1998).
43. M. J. Bloemer and M. Scalora, "Transmissive properties of Ag/MgF2 photonic band gaps," Appl. Phys. Lett. **72**, 1676–1678 (1998).
44. M. Scalora, M. J. Bloemer, A. S. Manka, J. P. Dowling, C. M. Bowden, R. Viswanathan, and J. W. Haus, "Pulsed second-harmonic generation in one-dimensional, periodic structures," Phys. Rev. A **56**, 3166–3174 (1997); J. W. Haus, R. Viswanathan, M. Scalora, A. G. Kalocsai, J. D. Cole, and J. Theimer, "Enhanced second-harmonic generation in media with a weak periodicity," Phys. Rev. A **57**, 2120–2128 (1998).
45. G. D'Aguanno, M. Centini, C. Sibilia, M. Bertolotti, M. Scalora, M. J. Bloemer, and C. M. Bowden, "Enhancement of $\chi^{(2)}$ cascading processes in one-dimensional photonic bandgap structures," Opt. Lett. **24**, 1663–1665 (1999); M. Centini, C. Sibilia, M. Scalora, G. D'Aguanno, M. Bertolotti, M. J. Bloemer, C. M. Bowden, and I. Nefedov, "Dispersive properties of finite, one-dimensional photonic band gap structures: applications to nonlinear quadratic interactions," Phys. Rev. E **60**, 4891–4898 (1999).